ELSEVIER

Coordination Chemistry Reviews
165 (1997) 447–474

COORDINATION CHEMISTRY REVIEWS

Phosphines as structural and functional probes of hemoproteins

Gérard Simonneaux *

Laboratoire de Chimie Organométallique et Biologique, URA CNRS 415, Université de Rennes 1, 35042 Rennes cedex, France

Received 24 January 1997

Contents

Abstract

The current application of phosphines as structural and functional probes of hemoproteins is reviewed, including iron porphyrin models. The biophysical studies performed to date on

* *Correspondence to: Gérard Simonneaux, Laboratoire de Chimie Organométallique et Biologique, UMR 6509, Université de Rennes 1, 35042 Rennes cedex, France.*

PII S0010-8545(97)00040-4

hemoproteins are discussed on the basis of the spectroscopic results obtained with models. A review with 126 references. © 1997 Elsevier Science S.A.

Keywords: Electron-transfer; Hemoproteins; Phosphines; Structure–function relationship

1. Introduction

The study of the binding of small ligands to heme proteins has played an important role in our ability to understand protein–substrate interactions in general [1]. Paralleling the progress in classical coordination chemistry have been the rapid advances made in the coordination chemistry of biomolecules [2,3]. Probably the most familiar examples of bioinorganic chemistry are the oxygen carriers such as hemoglobins. The simplicity of the ligands (O_2, CO, NO, CNR and CN^-) and the wealth of structural data available for heme proteins have led to a better understanding of these systems. Surprisingly, though there are numerous examples of complex compounds of trivalent phosphorus derivatives [4–6], the use of phosphines as structural and functional probes of hemoproteins has been hidden for a long time.

Indeed, the formation of the phosphorus trifluoride–hemoglobin complex was reported by Wilkinson in 1951 [7]. The purpose was to compare the complexation of carbon monoxide and phosphorus trifluoride, both ligands being considered as strong π acceptor ligands [6]. Unfortunately the stability of ligated PF_3 in hemoglobin was very short-lived (a few minutes) due to probable hydrolysis of the P–F bond. Thus, it is quite recently that biochemists and chemists have again begun to think about the possibility of introducing phosphines into biological material.

In this article, we review the recent developments of phosphine ligation to iron–porphyrin models and to heme proteins. To our knowledge, there is no reported review on this topic. One of the major applications of phosphine complexation has been in the study of iron porphyrin complexes in biological macromolecules both directly and in model systems. In the first two chapters, we will confine our attention to iron porphyrin models. Then the use of phosphines as structural and functional probes of hemoproteins will be presented.

2. Phosphines as ligands to iron porphyrin models

2.1. Ferroporphyrins

Several routes have been used to prepare bis(phosphine) and bis(phosphite) ferroporphyrins, all from reduction of ferriporphyrins. Different porphyrins can be used for these syntheses (Fig. 1). The reducing agent may be either sodium dithionite in dichloromethane/water [8], in toluene/water [9], zinc amalgam in toluene [10] (Fig. 2) or sodium borohydride in tetrahydrufuran (THF) [11]. Problems may be encountered due to incomplete reduction. In this case the reduction with $NaBH_4$ in

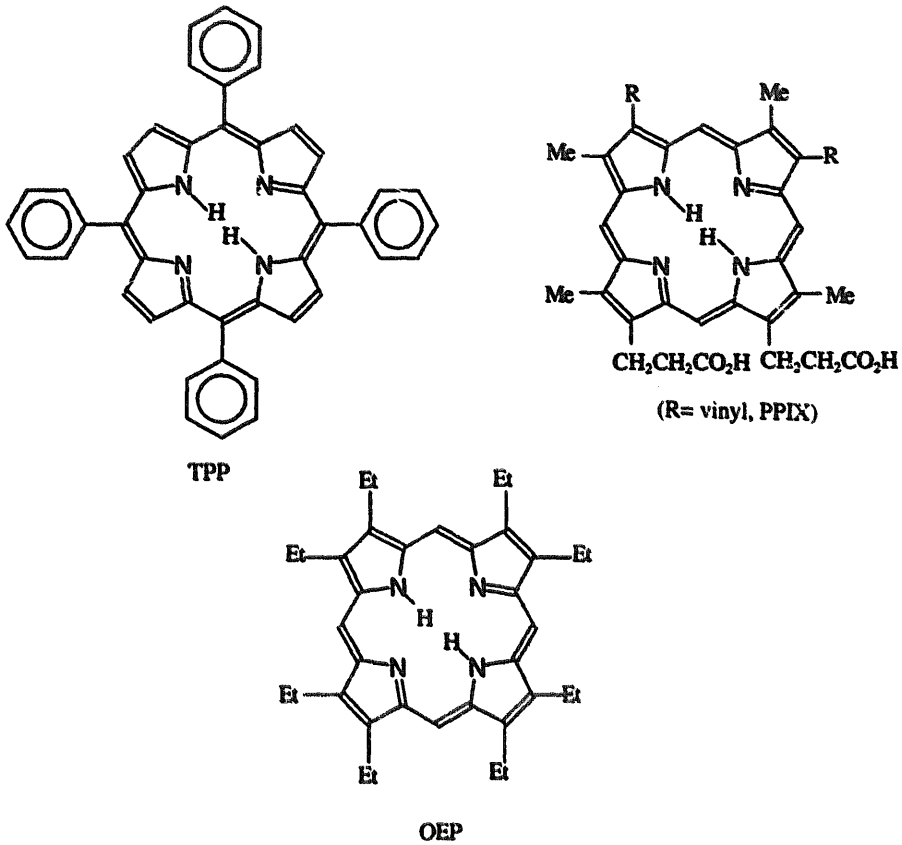

Fig. 1. Structures of common porphyrins: *meso*-tetraphenylporphyrin (TPP), octaethylporphyrin (OEP), protoporphyrin IX (R = vinyl, PPIX), deuteroporphyrin (R = H, DP) and mesoporphyrin (R = Et, MP).

THF seems more complete. The reaction can also be carried out with a large excess of ligand which presumably acts as the reducing agent [12,13]. Actually, autoreduction of ferric porphyrins by phosphines was previously reported in 1977 but no radical species was detected [14]. The bis(phosphine) complexes are quite stable in the solid state but react rapidly with traces of air in solution, although no characterizable complexes have been isolated [13]. However, ferryl porphyrins react with triphenylphosphine to give triphenylphosphine oxide and such ferryl intermediates may be involved in the reaction with oxygen [15]. $Fe(TPP)(PPh_3)_2$ has also been prepared, but not in a pure state [13]. The bis-phosphine ferrous porphyrins are all diamagnetic as expected for complexation of two strong field ligands with ferrous porphyrins [16]. Mixed-phosphine–carbonyl complexes of ferrous protoporphyrin IX dimethyl ester [9] and of ferrous tetraphenylporphyrins [10,11] have also been reported. The new carbonyl complexes $Fe(TPP)(CO)(PR_3)$ and $Fe(PXIDME)(CO)(PR_3)$ were obtained in situ by stirring CO-saturated methylene chloride solutions with the corresponding bis(phosphine) complexes. The reaction is reversible and the mixed-phosphine–carbonyl complexes have not been isolated. Solutions of $Fe(TPP)(PBu_3)_2$ also react rapidly with a variety of aromatic aldehydes at room temperature to yield $Fe(TPP)(PBu_3)CO$. The aldehyde decarbonylations involve radical pathways and become catalytic under argon in the presence of an

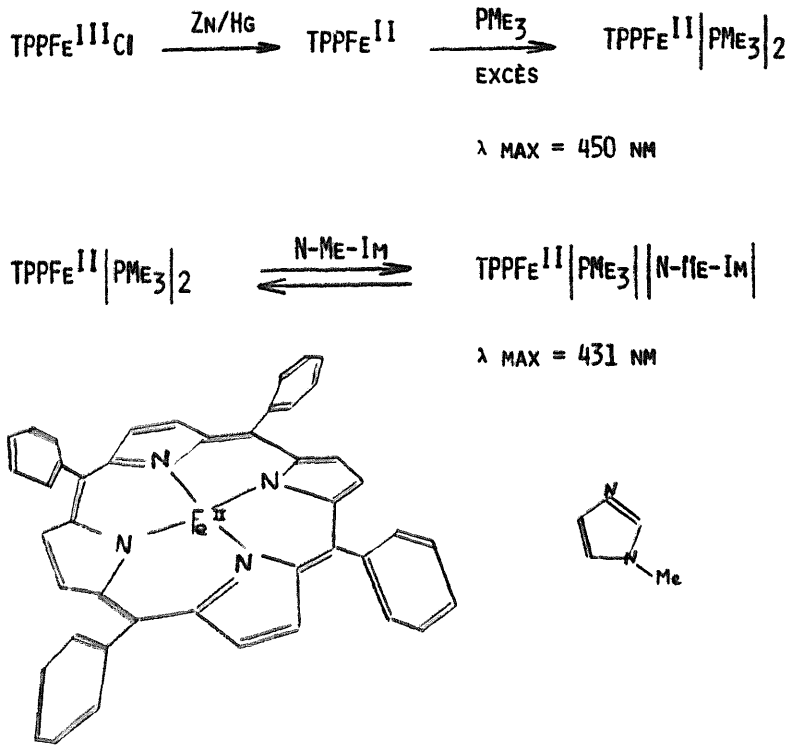

Fig. 2. Synthetic scheme for the preparation of phosphine iron(II)porphyrin complexes.

excess of aldehyde [13]. Mixed-phosphine–imidazole complexes of ferrous tetraphenylporphyrins have been also prepared as models of phosphine hemoglobin derivatives (Fig. 2) [10].

Equilibrium [9,13] and kinetic [9] investigations of phosphine and phosphite complexes of ferrous porphyrins have been described. Using standard spectrophotometric techniques, the equilibrium constant for CO binding to $Fe(TPP)(PBu_3)_2$ (Eq. (1)) is $K=0.65$ [13] and to Fe(protoporphyrin IX)$(PBu_3)_2$ is $K=1.7$ [9] in similar experimental conditions (23–25 °C, toluene). For other mixed-ligated ferrous porphyrins, the relative affinity order is $PBu_3 > P(OBu)_3 >$ MeIm *trans* to MeIm and indicates a strong Fe-phosphorus bond with small phosphines. The weak affinity with triphenylphosphine is probably due to the steric interaction between the phenyl groups of the porphyrin and the phenyl groups of the ligand.

$$Fe(TPP)(PBu_3)_2 + CO \overset{K}{\rightleftarrows} Fe(TPP)(CO)(PBu_3) + PBu_3 \qquad (1)$$

All the $Fe(TPP)(PR_3)_2$ complexes exhibited "hyper" UV-visible spectra with two Soret bands, one in the 450 nm region and the second in the near-ultraviolet 350 nm region [12]. A phosphorus to porphyrin charge-transfer transition $a_{2u}(\sigma_5-\sigma_6) \rightarrow e_g(\pi^*)$ may interact with the porphyrin $a_{1u}(\pi)$, $a_{2u}(\pi) \rightarrow e_g(\pi^*)$ transitions. This explains the optical feature, i.e. the red-shifted Soret-band. Such an interpretation has been previously proposed by Hanson et al. [17] for P450-CO and the same authors suggested that this phenomenon can be extended to heme complexation with other good electron donating ligands.

The ^1H NMR spectrum of the PMe_3 ligand in $Fe(TPP)(PMe_3)_2$ shows a signal at high field (−2.3 ppm). The high field shift is due to the shielding effect of the porphyrin ring current [10]. A similar upfield spectral feature is observed with the mixed species $Fe(TPP)(PMe_3)L$ (L = pyridine or *N*-methylimidazole) (Table 1). This remarkable property will be used to probe the active site of the hemoproteins because coordination of trimethylphosphine to the iron will give a signal outside the bulk of the protein resonances [18] (see below)). The ^1H NMR spectrum shows also a group of signals corresponding to the porphyrin ring protons and the pyrrole protons (7–9 ppm). The chemical shifts of the latter are very similar to those of $Fe(TPP)(pyr)_2$ [19] and are expected for diamagnetic iron(II) porphyrin derivatives [20,21].

^{31}P NMR shifts have also been reported for $Fe(TPP)(PR_3)_2$ [10,22] and $Fe(TPP)(PR_3)$(base) complexes (base: imidazole, pyridine, benzyl methyl sulfide, cyanopyridine...) [10,11,23] (Table 1). The ^{31}P NMR spectra of complexes $Fe(TPP)(PR_3)_2$ exhibit two sharp peaks in the presence of excess phosphine: a signal due to free phosphine and a signal due to the bound phosphine. This implies slow ligand exchange on the NMR time-scale under the experimental conditions used. It was found that the ^{31}P chemical shifts are sensitive to the electron density on the metal and consequently to the nature of both the porphyrin and the *trans* axial ligand. For example, a chemical shift difference of 3.5 ppm is seen in the deprotonation of the imidazole complex $Fe(TPP)(PMe_3)$(Him) [10]. The strong *trans* effect can be related to the sensitivity of the PMe_3 ligand to the electronic variation around the iron atom. Of particular relevance to this study on hemoproteins is the observation that the proximal ligand in horseradish peroxidase is thought to be a histidyl residue that is strongly bonded to another amino acid at the imidazole 1-H site giving it imidazolate character [24]. However, care is necessary in these studies because traces of paramagnetic porphyrins will also modify the chemical

Table 1
^1H and ^{31}P NMR data for $Fe(TPP)(PR_3)L$ complexes[a]

Complex	Porphyrin			PR_3		
	pyr	*ortho*	*meta* and *para*	^1H[b]	^{31}P[c]	T (°C)
$Fe(TPP)(PMe_3)_2$	8.21	7.91	7.53	−2.61	13.5	25
$Fe(TPP)(PMe_2Ph)_2$	8.19	7.82	7.55	−2.45[d]	14.5	25
$Fe(TPP)(PMe_3)$(MeIm)	7.89	7.78	7.49	−2.87[e]	25.5	−40
$Fe(TPP)(PMe_3)$(Py)	8.40	7.41	7.26	−2.93[f]	25.7	−40
$Fe(TPP)(PMe_3)$(Im)	–	–	–	–	23.7	−40[g]
$Fe(TPP)(PMe_3)(Im^-)$	–	–	–	–	20.2	−40[g]

[a] 0;05M in deaerated CD_2Cl_2 containing an excess of phosphine L.
[b] In ppm; Me_4Si reference.
[c] In ppm; H_3PO_4 (85%) reference.
[d] Ph: *o*, 4.26 (d); *m*, 6.43 (t); *p*, 6.75 (m).
[e] MeIm: data were not determined.
[f] Py: *o*, 2.49 (d); *m*, 5.43 (t); *p*, 6.14 (t).
[g] Solvent: DMF.

shift [11]. The use of ^{57}Fe decoupling of the ^{31}P signals of PMe_3-coordinated ^{57}Fe enriched porphyrin complexes has been recently reported in order to determine the chemical shifts of ^{57}Fe [11,23]. The method utilizes the sensitive ^{31}P nucleus as the detected signal. The scalar coupling of ^{57}Fe to the ^{31}P nucleus of PMe_3, which resulted in the observed doublet, is then decoupled to detect the frequency necessary to collapse the Fe–P doublet in the ^{31}P NMR spectrum, using a double resonance technique. This method is very useful since the ^{57}Fe NMR signals are very difficult to detect due to very large chemical shift range and very low sensitivity of the ^{57}Fe nucleus.

A comparative Mössbauer investigation of low-spin iron(II) porphyrin complexes with bis(phosphine) or bis(phosphite) axial ligands was first reported by of Ohya et al. [12]. Upon replacement of the axial ligands PR_3 by $P(OR)_3$, the porphyrin appears to be able to modify the σ and π bonding characteristics to follow the requirements of the axial ligands. The results supported the existence of an electron sink effect capability of the macrocyclic ligand to explain a larger quadrupole splitting for phosphine derivatives than for phosphite derivatives. A relationship between these ^{57}Fe NMR chemical shifts and the Mössbauer quadrupole splitting in a series of various phosphine, imidazole and pyridine ligated complexes has been proposed very recently [25]. The authors emphasize the value of the Mössbauer–NMR correlation to detect the ^{57}Fe NMR signals in these systems.

Resonance Raman spectra are reported for phosphine and phosphite derivatives of iron mesoporphyrin IX [8]. π-acid ligands such as phosphites or aromatic phosphines shift porphyrin bands I, III and V to higher frequencies as do CO and O_2 but with a smaller influence. A correlation between the increased π-acidity of the ligand and the increased position of these bands has been found and related to a decrease in π electron back-donation from iron d_{xz} and d_{yz} orbitals to the π^* antibonding porphyrin orbitals [8].

The crystal and molecular structures of several derivatives: $[TPPFe(PMe_2Ph)_2]$ (Fig. 3) [10], $TPPFe(P(n\text{-}Bu)_3)_2]$ [13], $[(p\text{-}OCH_3)_4TPPFe(PMe_3)_2]$ [11], $[OEPFe(PMe_3)_2]$ [11] have been determined by X-ray crystallography (TPP is tetraphenylporphyrin and OEP is octaethylporphyrin). The porphyrinato core is essentially planar and the Fe–N distances average from 1.990(6) to 1.999(6) Å as expected for low-spin iron(II) porphyrins [15]. The axial trimethylphosphine ligands have their methyl groups in staggered conformation. The Fe–P distances range from 2.275(6) to 2.346(1) Å. These distances are longer than those observed in the analoguous phosphite iron(II) complex $T(p\text{-}OMe)PPFe[(P(OMe)_3]_2]$ (2.255(2) Å) [26]. This is consistent with a greater π-acceptor ability of phosphite ligands compared with that of phosphine ligands [27] with a concomitant increase in π back bonding from iron to the axial ligand.

2.2. *Ferriporphyrins*

A major difficulty that is encountered with phosphine complexation to the ferric state is the autoreduction of ferric porphyrins [14]. As an example, addition of PMe_3 to tetraphenylporphyrin ferric chloride FeTPPCl at room temperature yielded

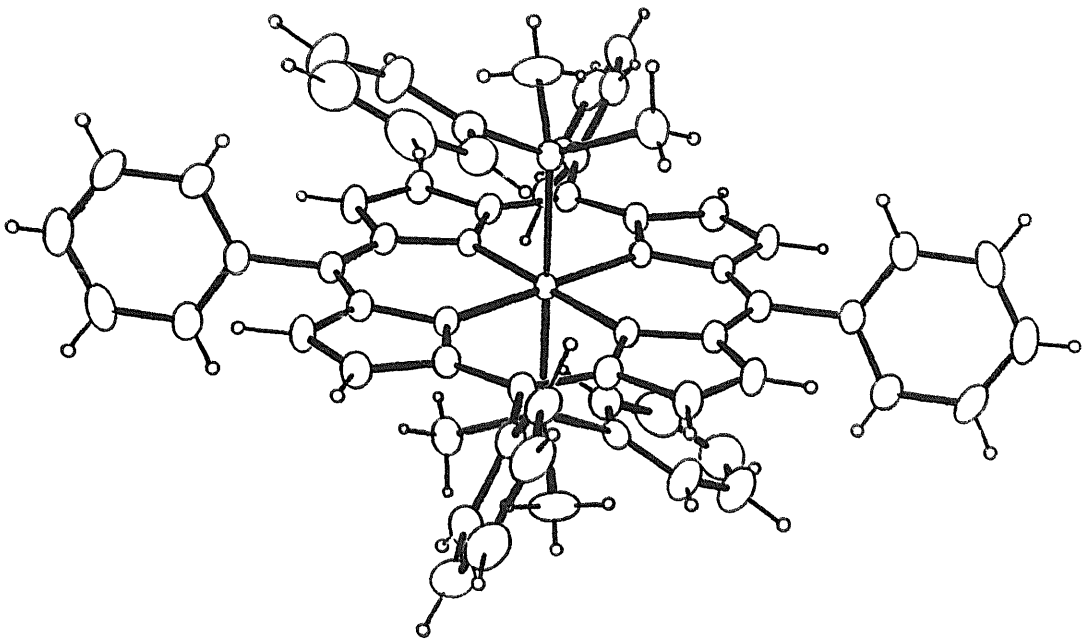

Fig. 3. A perspective view of the $Fe(TPP)(PMe_2Ph)_2$ molecule (adapted from Ref. [10]).

directly to $FeTPPP(PMe)_2$ [28]. Thus the general strategy [29–31] for preparation of phosphine and phosponite derivatives is to choose *meso*-tetraphenylporphyrinato iron(III) ligated by weakly coordinating counterions (perchlorate or triflate) [32,33], as intermediates which made possible product isolation (Eq. (2)).

$$Fe(TPP)ClO_4 + 2(PR_3) \rightarrow Fe(TPP)(PR_3)_2ClO_4 \quad (2)$$

$$Fe(TPP)(1-MeIm)_2ClO_4 + (PR_3) \rightarrow Fe(TPP)(1-MeIm)(PR_3)ClO_4 \quad (3)$$

Complexes with natural porphyrins can be prepare in the same way using deuteroporphyrins as the macrocyclic ligand [29]. It should be noted that a second difficulty that is encountered in preparing ferric derivatives with phosphonites, which are less basic ligand than phosphines, is the necessity of adding a large excess of the ligand to assure complete complexation [31]. Using perchlorate or trifluoromethyl sulfonate as an intermediate allows also to solve the autoreduction problem. Mixed-ligation complexes can be prepared with ferric tetraphenylporphyrins by addition of PMe_3 to $Fe(TPP)(Py)_2ClO_4$ or to $Fe(TPP)(1\text{-}MeIm)_2ClO_4$ (Eq. (3)) [29] and, with dimercaptide hemin derivatives, by addition of an excess of diethylphenylphosphine at low temperature [34,35].

The $Fe(TPP)(PR_3)_2ClO_4$ complexes exhibited hyperspectra with two Soret bands, one in the 440 nm region and the second in the near-ultraviolet region (360 nm). It is interesting to note that two phosphines are necessary for the hyperporphyrin spectrum since mixed ligated species with one phosphine and one nitrogenous base exhibited normal spectra. Hyperporphyrin spectra for bis-mercaptide and mercaptide phosphine hemin complexes are two other exceptions [34,35].

Progressive addition of PMe_3 to $Fe(TPP)OClO_3$ has been followed by UV-

visible and ^1H NMR [28]. A mono phosphine intermediate formulated as (Fe(TPP)(PMe)$OClO_3$) can be detected and characterized by a Soret band at 415 nm and signals at 6.6 (*p*-phenyl), 5.67 (*o*+*m*-phenyl), −18.9 (pyrrole) and −20.8 ppm (PMe_3) in the ^1H NMR spectrum. Accordingly, a low-spin-state can be proposed for this intermediate. As previously suggested [36], a mono addition is possible since the intermediate spin starting complex, as Fe(TPP)$OClO_3$, already has partial spin pairing.

The room-temperature ^1H NMR data of bis-phosphine/iron(III) porphyrins (PMe_3, PMe_2Ph) and mixed-ligated iron porphyrins are characteristic of the low-spin state ferric porphyrin system (Eq. (3)) [29]. All the phosphine complexes have pyrrole resonances between −19 and −21 ppm. These chemical shifts are typical of iron(III) tetraarylporphyrins in a low-spin state [37–41]. As an example, the ^1H NMR spectrum of Fe(TPP)(PMe_3)(1-MeIm)ClO_4 is shown in Fig. 4. In order to characterize the electronic ground state of the phosphine iron porphyrins, analysis of the chemical shifts was made according to empirical methods (Table 2) [40,41]. The data indicate that the *meso*-phenyl shifts are totally dipolar in origin for the Fe(TPP)(PMe_3)(1-MeIm)ClO_4 complex but with a small contact contribution for Fe(TPP)(PMe_3)$_2ClO_4$ [29]. The large upfield pyrrole proton contact shifts agree with electron transfer from the porphyrin $3e_\pi$ orbitals to the d_{xz} and d_{yz} orbitals of the metal [40,41]. The Curie plots are linear for all the protons of the porphyrin ligand, indicating a simple electronic ground state. The isotropic shift obtained for PMe_3 is slightly upfield due to a contact shift and a dipolar shift which have a similar magnitude but opposite signs. A dramatic change is observed with the Fe(TPP)(PMe_3)(1-MeIm)ClO_4 complex. In comparison to that in the bis(phosphine) species, the PMe_3 proton signal is at higher field (−10 ppm), implying that the contact shift dominates. The π-acceptor character of the phosphorus ligand, due to the presence of empty 3d orbitals, has a very large effect on the observed isotropic shifts of the axial ligand protons. Consequently PMe_3 in low-spin ferric hemoproteins will resonate upfield of the diamagnetic region, irrespective of the nature of the

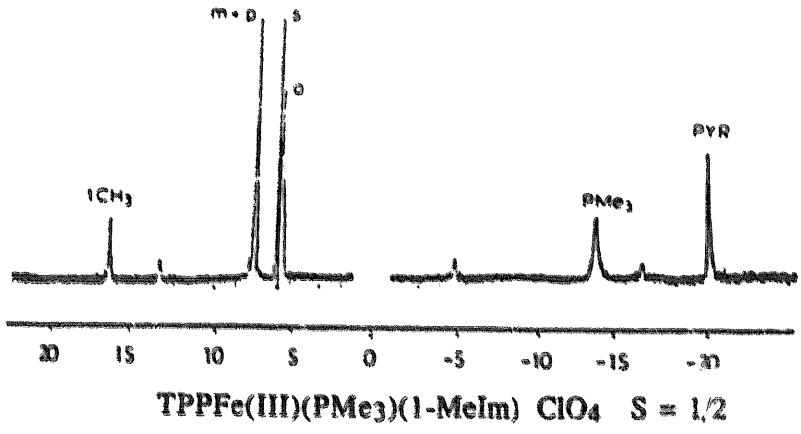

Fig. 4. ^1H NMR spectrum of Fe(TPP)(PMe)(1-MeIm)ClO_4 in CD_2Cl_2 at 20 °C. Assignments of various resonances are indicated (S marks the residual solvent peaks).

Table 2
Observed chemical shifts and separation of the isotropic shift into contact and dipolar contribution in $Fe(TPP)(PMe_3)_2ClO_4$ and $Fe(TPP)(PMe_3)(1\text{-MeIm})ClO_4$

Proton type	$Fe(TPP)(PMe_3)_2ClO_4$				$Fe(TPP)(PMe_3)(1\text{-MeIm})ClO_4$			
	$(\Delta H/H)^a$	$(\Delta H/H)^b_{iso}$	$(\Delta H/H)_{dip}$	$(\Delta H/H)_{con}$	$(\Delta H/H)^a$	$(\Delta H/H)^c_{iso}$	$(\Delta H/H)_{dip}$	$(\Delta H/H)_{con}$
o-H	5.00	−2.91	−2.16	−0.75	5.03	−2.75	−2.77	0
m-H	6.78	−0.75	−0.92	+0.23	6.26	−1.23	−1.26	0
p-H	6.36	−1.17	−0.82	−0.29	6.2	−1.23	−1.13	0
pyrr-H	−19.6	−27.81	−4.08	−23.73	−19.45	−27.34	−5.24	−22.10
PMe_3	−5.00	−2.39	+10.93	−13.32	−12.95	−10.08	14.05	−24.10
Me(Im)					15.03	13.43	6.12	7.31
CH(Im)					12.18			
					−4.99			
					−15.72			

[a] Chemical shift in ppm at 20 °C with Me_4Si as internal reference (CD_2Cl_2).
[b] Isotropic shift with diamagnetic $Fe(TPP)(PMe_3)_2$ complex as Ref. [10].
[c] Isotropic shift with diamagnetic $Fe(TPP)(PMe_3)(1\text{-MeIm})$ complex as Ref. [10].

protein and thus, could serve as a probe of the active site (see below). The ^{31}P chemical shift of $Fe(TPP)(PMe_3)_2ClO_4$ has been also reported (36 ppm) [11].

The EPR g values reported for $Fe(TPP)(PMe_3)_2ClO_4$ are $g=2.687$, 2.088 and 1.680 at 140 K [29]. These g values are familiar for low-spin ferric porphyrins [34,35,42–46]. However, at 8 K the only EPR signal present is a large g_{max} signal at $g=3.5$ [41]. This signal is consistent with near degeneracy of the d_{xz} and d_{yz} orbitals as expected for low-spin ferric complexes with axial ligands that have effective cylindrical symmetry [41].

It should be noted that the ^1H NMR and EPR studies of low-basicity phosphonite derivatives, $Fe(TPP)[P(OR)_2Ph]_2ClO_4$ (R = Me, Et), which stabilize the unusual electronic ground state $(d_{xz},d_{yz})^4$ $(d_{xy})^1$, have also been reported [31]. In this particular case, a large π-spin delocalization to the *meso*-position and an anti-Curie behavior of the pyrrole protons is observed. A similar situation was also observed with the low-spin complex as $Fe(TPP)(4\text{-CNPy})_2ClO_4$ [47a] and $Fe(TPP)(t\text{-BuNC})_2ClO_4$ [47b].

The crystal and molecular structures of one complex: $[TPPFe(PMe_2Ph)_2]$ ClO_4 [48], has been determined by X-ray crystallography (Fig. 5). The porphyrinato core is essentially planar and the Fe–N distances average to 1.999(6) Å as expected for low-spin iron(III) porphyrins [16]. The axial trimethylphosphine ligands have their methyl groups in staggered conformation. The Fe–P distance is 2.350(1) Å. This distance is longer than that observed in the analogous phosphine iron(II) complex (2.284(1) Å). The crystal and molecular structures of $Fe(TPP)[(POR)_2Ph]_2ClO_4$ are completely different and show that the porphyrin ring is strongly ruffled, in agreement with the unusual $(d_{xz},d_{yz})^4$ $(d_{xy})^1$ electronic state [49]. This is consistent with a greater π-acceptor ability of phosphonite ligands compared with that of phosphine ligands [27] with a concomitant increase in π back bonding from iron to the axial ligand.

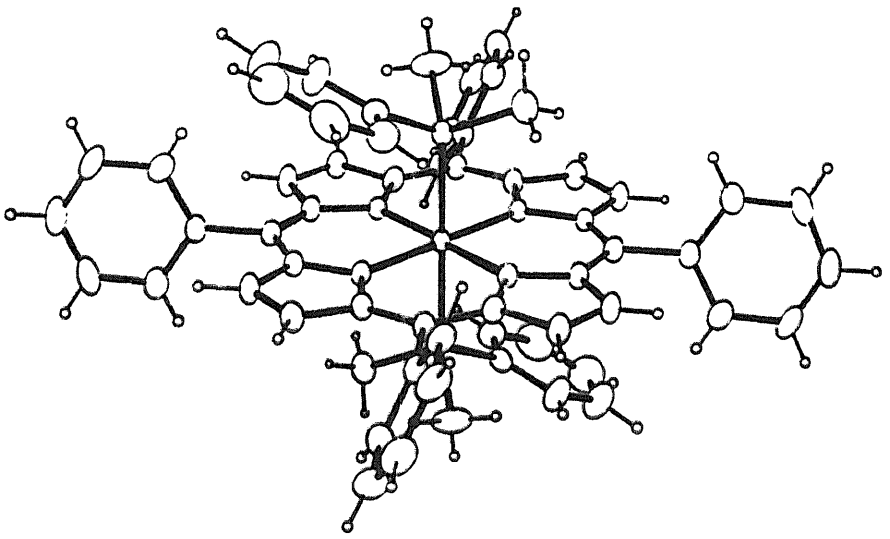

TPPFe(III)(PMe_2Ph)$_2$ ClO_4

Fig. 5. A perspective view of the Fe(TPP)(PMe_2Ph)$_2ClO_4$ molecule (adapted from Ref. [48]).

3. Phosphine binding as a structural probe of hemoprotein active site

In 1951 Wilkinson first reported complexation of trifluorophosphine with reduced hemoglobin [7]. No more was heard for over twenty years until Mansuy et al. provided conclusive evidence in 1974 that organic phosphines are highly potent ligands for cytochrome P-450 of rat liver microsomes [50]. Since then, a number of papers relating to the complexation of alkyl and aryl phosphines to hemoproteins have appeared including myoglobins (Fig. 6) [18,22,51–56], hemoglobins [18,22,52–56], bacterial and microsomal cytochromes P-450 [50,51,57–60], and peroxidases [51,58,61]. For clarity, we will review separately in this section each main hemoprotein group from the structural point of view. Unfortunately, no X-ray structure of a phosphine ligated hemoprotein has been reported.

3.1. Myoglobin and hemoglobin

3.1.1. Fe(II)

Addition of PMe_3 to reduced horse heart myoglobin [62] immediately gave a phosphine myoglobin complex characterized by its electronic spectrum (λ = 436, 534 and 568 nm) (Fig. 7) [22]. This formation does not imply any protein denaturation, since CO bubbling to the solution of Mb PMe_3 for 2 mn gave carbon monoxide complexation to myoglobin [22] which produced a spectrum typical of Mb CO [1]. Similar results have also been obtained with sperm whale myoglobin and hemoglobins from a variety of sources [22,52] (Fig. 8).

$$Mb + PMe_3 \rightleftharpoons MbPMe_3 \quad (4)$$

The binding of phosphines to ferrous myoglobin is characterized by high affinity.

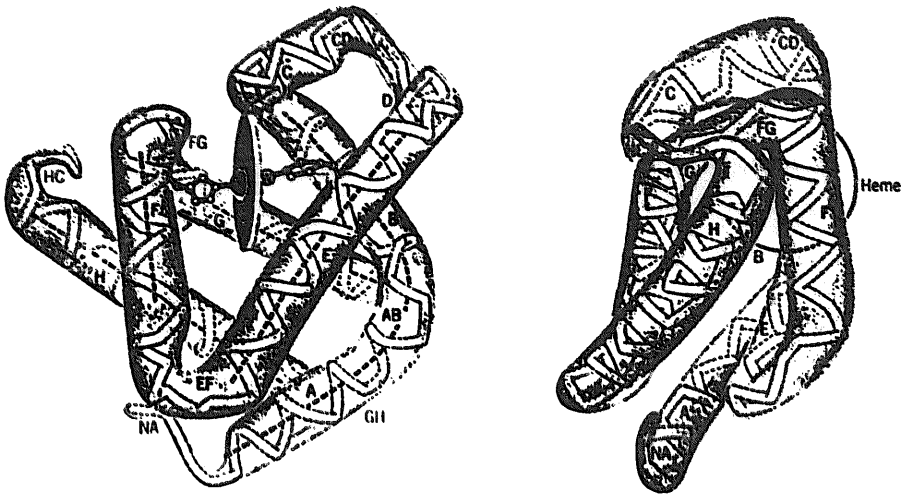

FRONT VIEW SIDE VIEW

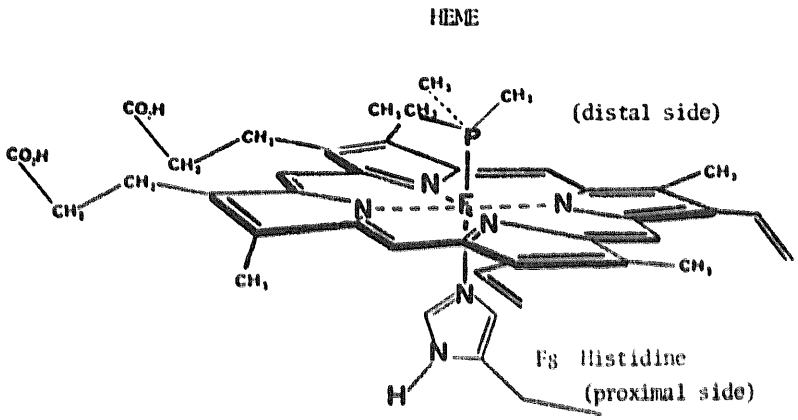

Fig. 6. Schematic representation of the trimethylphosphine complexation to myoglobin (adapted from Ref. [62]).

The equilibrium dissociation constants are 1.2 μM for horse heart myoglobin and 1.1 μM for sperm whale myoglobin (Eq. (4)) [56]. It may be noticed that the affinity of myoglobin for CO is much higher (40-fold) than for PMe_3 but that the affinity for oxygen and trimethylphosphine is quite similar [63]. Association and dissociation rate constants were also measured for trimethylphosphine binding to myoglobins [56] and it was concluded that the high affinity is mainly due to very low kinetic dissociation constants ($k_{off} = 7.7$ mM) related to the strong phosphorus–iron bond. In contrast, only small association constants were observed for ligand binding to myoglobins, as expected for the migration and ligation of a bulky ligand into the distal pocket.

The ^1H NMR study of PMe_3 bound to iron(II) is very characteristic since it

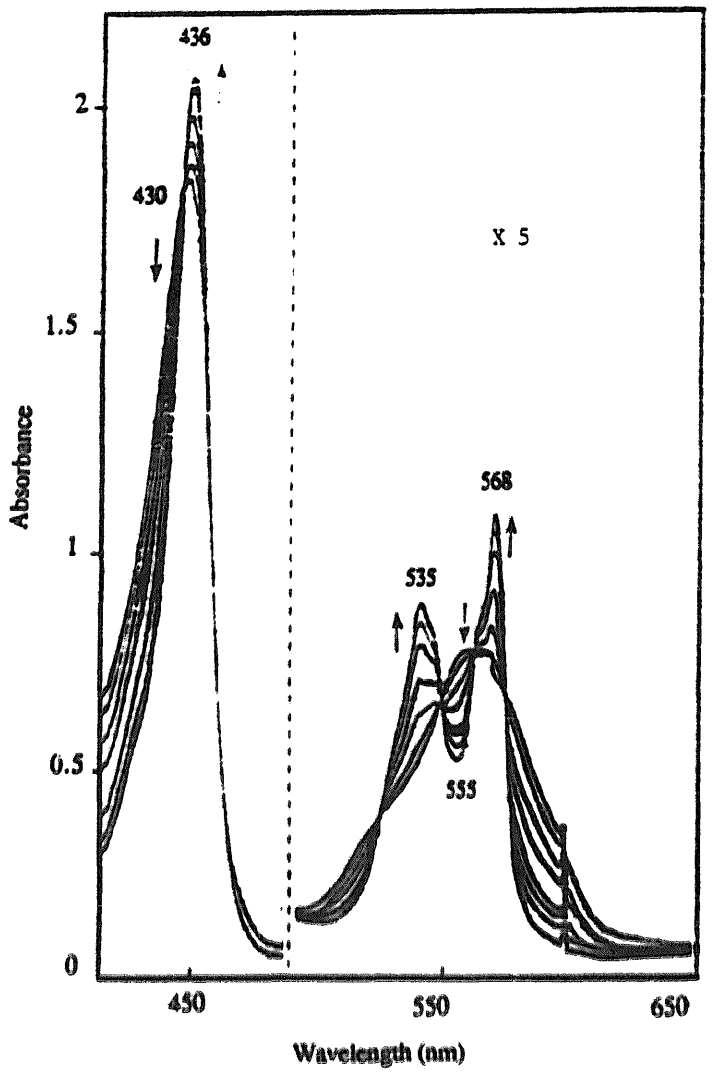

Fig. 7. Spectrophotometric titration of ferrous myoglobin with trimethylphosphine in 0.1M potassium phosphate, pH 7.15 and at 25 °C.

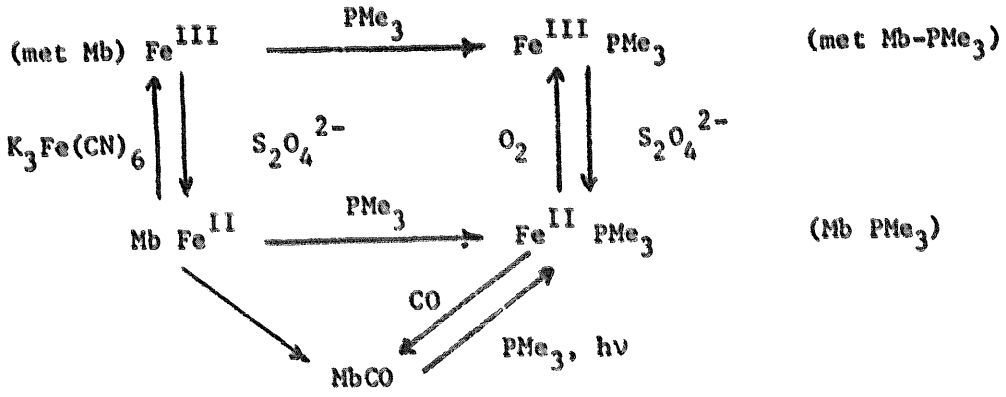

Fig. 8. Synthetic scheme for the complexation of trimethylphosphine to myoglobin.

exhibits a resonance at high field (−3.5 ppm) (Fig. 9) [53,54] which was assigned to the axial ligand by using $P(CD_3)_3$ instead of PMe_3 [29]. Thus the ligand appears well away from the bulk of the diamagnetic protein resonances due to the shielding effect of the ring current shift of the porphyrin. The comparison of the chemical shift of PMe_3 bound to myoglobin with those of ferrous porphyrin models suggests a low-spin ferrous state (see above) and shows that the ligand is very sensitive to the protein environment of the heme. This chemical shift sensitivity is confirmed by the ^1H NMR study of human adult hemoglobin where two resonances corresponding

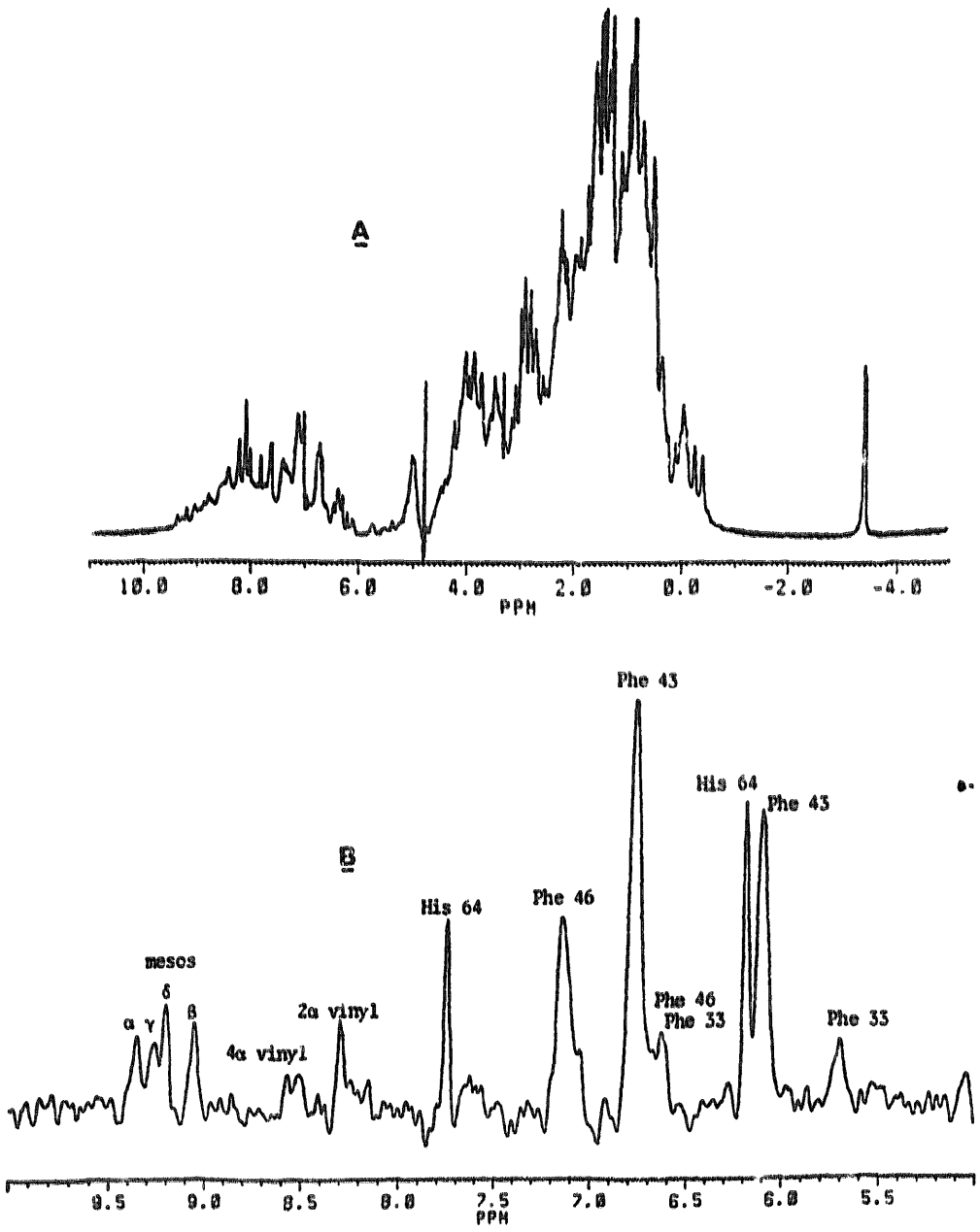

Fig. 9. (a) ^1H NMR spectrum of trimethylphosphine myoglobin (pH 5.6, 25 °C). (b) Row from NOESY spectrum of $MbPMe_3$, showing NOE connectivities involving aromatic protons around the PMe_3 protons (adapted from Ref. [54]).

to PMe_3 bound to the heme of α and β chains are observed [18]. The use of this ligand as a structural probe is also demonstrated by perturbations in the heme pocket induced by a thiol reagent which have been detected in ^1H spectra [52]. The ^{31}P NMR technique is quite complementary since separated signals can also be observed for PMe_3 bound to the α and β chains of hemoglobins [18].

Two-dimensional nuclear magnetic resonance techniques were used to assign resonances corresponding to heme pocket and several other residues of horse heart and sperm whale myoglobins ligated by trimethyl phosphine [54,56]. Two-dimensional nuclear Overhauser effect spectroscopy [NOESY] [64] has been recognized as a very powerful method for investigating the conformation of biological macromolecules in solution [65]. However, in unfavorable cases, this technique is of somewhat limited scope because of the difficulty of obtaining reliable assignments of the NMR resonances in the crowded area in such a large protein. The highfield shifts of PMe_3 proton resonances (−3.4 ppm) removed this difficulty because these resonances are markedly upfield and well away from the bulk of the diamagnetic protein resonances. The assignment procedure was based mainly on the nuclear Overhauser effect connectivities (from NOESY spectra) with the ligand and the heme substituents (Fig. 9). Some assignments were also obtained using the phase-sensitive and double-quantum filtered ^1H–^1H correlated spectra (DQF-COSY) [66]. For quantitative measurements of Overhauser effects, application of truncated driven NOE techniques [67] between protons of distal residues and the methyl groups from the ligand was used to determine internuclear distances. These results have permitted the mapping of the heme pockets and investigating the conformational differences in the heme pockets between horse heart and sperm whale myoglobins. The interprotein distances between distal amino acid residues and PMe_3 were found to be longer in horse heart myoglobin relative to those in sperm whale myoglobin. This result suggests that the size of the heme pocket is larger in horse heart myoglobin [56].

3.1.2. Fe(III)

Phosphines are more versatile than CO in that they may serve as ligands to both the ferric and the ferrous iron of hemoproteins. Addition of PMe_3 to horse heart metmyoglobin immediately gave a phosphine myoglobin complex characterized by its electronic spectrum ($\lambda = 370$, 424 and 536 nm) [53]. Complexations of bis(hydroxymethyl)methylphosphine and dimethylphenylphosphine to metmyoglobin have also been reported [51].

As in the ferrous state, the ^1H NMR study of PMe_3 bound to metmyoglobin is very characteristic since it exhibits a resonance at very high field (−12 ppm). Thus the ligand appears well away from the bulk of the diamagnetic protein resonances due to the paramagnetic effect. The comparison of the chemical shifts of heme methyl resonances with those of the metcyano complex of sperm whale [68] and horse heart [69] myoglobins suggests a low-spin ferric state. The chemical shift sensitivity, observed in the ferrous state, is maintained in the ferric state since in the ^1H NMR spectrum of human adult methemoglobin, two resonances corresponding to PMe_3 bound to the heme of α and β chains are observed [53]. ^1H NMR saturation transfer spectroscopy [67] and the nuclear Overhauser effect have been

utilized to assign several heme methyl and heme 2-vinyl group resonances [55]. A qualitative interpretation involving the heme methyl shift pattern in MetMbCN [70], metMbN_3, imidazole metMb [71] and trimethylphosphine metMb [55] shows a reverse methyl shift between pyrrole I and pyrrole IV. The different hyperfine shift pattern for the latter may originate from a possible reorientation of the proximal histidine plane or of the heme itself, different heme peripheral contact at the pyrrole I and IV, or a small contribution from high-spin character as was previously suggested for the other ligands [72–75]. The 2-vinyl group is formed in the *cis* configuration [55].

3.2. Cytochrome P-450 and chloroperoxidase

Phosphines bind to both ferric and ferrous P-450 [50,51,57–60] as well as to ferric heme-thiolate model complexes [34,35] producing hyperporphyrin spectra. Such a unique Soret band (>450 nm) has been shown to be characteristic of the presence of an axial endogeneous thiolate to the heme iron in both the ferric and ferrous state of the protein. Thus, phosphine binding is a structural probe of the active site since a similar feature is absent after phosphine ligation to myoglobin. This was first suggested by Mansuy et al. [50] and latter confirmed by Dawson et al. on cytochrome P-450cam [57], rabbit liver microsomal cytochrome P-450_{LM2}[59] and chloroperoxidase [51]. Moreover, magnetic circular dichroism studies of low-spin ferric cytochrome P-450 ligand complexes and chloroperoxidase complexes with dimethylphenylphosphine *trans* to cysteinate demonstrate that the spectrum fits into the hyperporphyrin category, with two MCD bands for each ultraviolet-visible absorption band [57].

The ^{1}H NMR studies of PMe_3 bound to ferric and ferrous P-450 are very characteristic since each spectrum exhibits a resonance at very high field: −10 ppm for ferric P-450 and −3.1 ppm for ferrous P-450 [76]. Thus the ligand appears well away from the bulk of the diamagnetic protein resonances by the paramagnetic effect. The comparison of the chemical shift of heme methyl resonances with those of the metcyano complex of the sperm whale [68] also suggests a low-spin ferric state.

Electron paramagnetic resonance investigations of exogeneous phosphine complexes of both proteins show EPR parameters that are quite comparable (P-450, $g=2.51$, 2.28 and 1.86; chloroperoxidase: $g=2.59$, 2.29 and 1.82 with bis(hydroxylmethyl)methylphosphine) [51,58,61]. These studies provided additional support for endogeneous thiolate ligation to the heme iron of chloroperoxidase since the ligation of the cyteine thiolate to iron of P-450 was already established at this time. Surprisingly cytochrome P-420_{LM2} [59] gave almost the same spectrum with diethylphenylphosphine as cytochrome P-450_{LM2}. Bis(phosphine) derivatives [59] or P-420 to P-450 reconversion were suggested [77].

3.3. Cytochrome c

It is well known that the iron–sulfur bond is weak in the oxidized state of cytochrome *c* and the axial methionine is easily displaced by various ligands, such

as cyanide [78–81], pyridine [82] and imidazole [83]. In contrast, it has been recognized for some time that the thioether sulfur bond of axial methionine is very strong in the reduced state of the iron [78,79,84]. In order to make possible the binding of trimethylphosphine to ferrocytochrome *c*, it was first thought that the methionine-80 sulfur atom must be alkylated in order to displace this ligand from the sixth coordination position in both oxidation states [85,86]. Thus the binding of trimethylphosphine to the axial position of the heme iron in modified cytochrome *c* by alkylation of methionine (cyt. *c* DMC) was first studied by nuclear magnetic resonance spectroscopy [87]. In order to make possible the binding of ligands to native ferrocytochrome *c*, it was decided later, to substitute the methionine by the ligand in the ferric state of the protein, and then to reduce the complex to the ferrous state [88]. Addition of trimethylphosphine to ferricytochrome *c* followed by reduction yielded a stable ferrous adduct ($t_{1/2} > 12$ h) characterized by its electronic spectrum, $\lambda = 424$, 527 and 554 nm and its ^{1}H NMR spectrum (Fig. 12). This latter is very similar to the spectrum obtained after addition of PMe_3 to cytochrome *c* DMC [87].

We must comment on the stability of the ferrocytochrome *c* PMe_3. Such a situation is rather unusual. In ferric cytochrome *c*, cyanide and imidazole displace the methionine whereas substitution of this aminoacid is not observed when the iron is reduced [89]. The hypothesis that the iron–methionine sulfur bond is enhanced by delocalization of the metal t_{2g} electron into the empty 3d orbitals of the sulfur atom in the ferrous state was suggested by Schejter and colleagues to explain this stability [86]. The relative stability observed with the phosphine may be related to the large steric effect due to the presence of the bulky phosphine ligand [90] which prevents the binding of the methionine [88].

4. Phosphines as functional probes of hemoproteins

4.1. Allostery

The affinity of trimethylphosphine for hemoglobin has been determined and the plot of the fractional saturation versus the concentration of unbound ligand is represented in Fig. 10 [18]. As expected, the equilibrium data exhibit markedly cooperative behavior as evidenced by the sigmoid nature of the binding curve and a large Hill coefficient ($n = 2.3$). Direct observation of intermediate ligation states of hemoglobin was possible using the ^{31}P NMR spectrum of partially liganded Hb as a probe. This spectrum contains resonances at normal chemical shift positions of the fully liganded species (R state), in addition to two resonances at intermediate positions. Analysis of the ^{1}H NMR results in the absence and in the presence of inositol hexaphosphate, which is known to bind between the β chains of deoxyhemoglobin and stabilize the T state [91], indicated that the intermediate resonances represent the PMe_3 bound to α subunit(s). Such a conclusion was confirmed by ^{31}P NMR investigations of trimethylphosphine binding to [Fe(II),Mn(II)] hybrid hemoglobin [92]. In 1970, using X-ray structure evidence, Perutz suggested that α

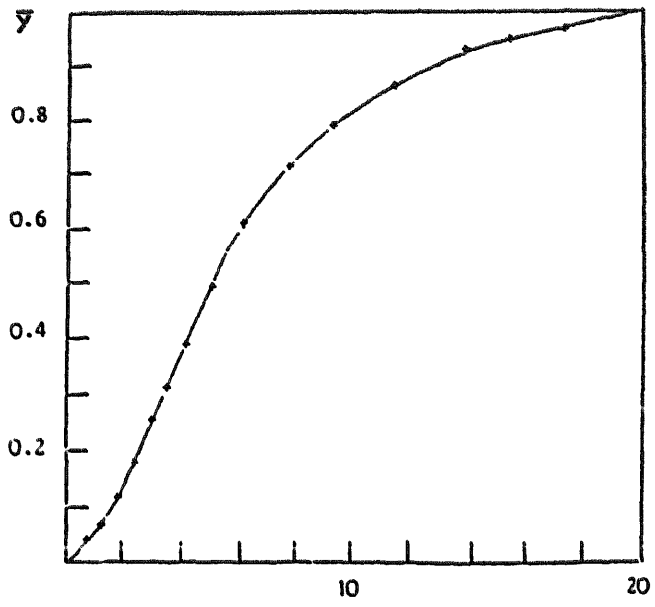

Equilibrium curve for PMe_3 binding to Hb

$$K = \frac{(HbL)}{(Hb)\,(L)^n}$$

n (Hill coefficient)
n = 2.8 (O_2) Hb
n = 2.3 (PMe_3) Hb

Fig. 10. Observed equilibrium curve for the binding of trimethylphosphine to hemoglobin in 0.1M tris-HCl at pH 7.1, 20 °C (adapted from Ref. [18]).

chains have a higher affinity for the ligands where hemoglobin is in the T state [93]. This strong preferential binding to α subunit(s) with respect to the β subunits in the T state was also supported by crystallographic studies of half oxygenated crystals which show a T state hemoglobin with oxygen bound to the α subunits but not to the β subunits [94]. The accumulation of more ligation intermediates in the binding of phosphines to hemoglobin than in the binding of oxygen was related to a smaller Hill coefficient in the former case [18].

4.2. Mechanism of electron transfer

4.2.1. Myoglobin and cytochrome c

Long range electron transfer is an essential component of biological systems, and much current research is centered around probing what factors control the rates of electron transfer [95]. Few studies of redox reactions of the oxygen carriers [96,97], hemoglobin and myoglobin, have been undertaken in part because suitable reduced

and oxidized states have not been available. Even though hemoglobin and myoglobin are not involved in electron transfer reactions, an understanding of the mechanism of a self-exchange reaction involving these proteins is important to the understanding of the overall picture of electron transfer processes in heme proteins. Several considerations make the trimethylphosphine/myoglobin system an excellent candidate for such analysis. First, a large body of functional data is already available [1] and the three-dimensional structure of *met*-myoglobin has been determined [98]. Second, trimethylphosphine (PMe_3) may serve as a ligand to both the ferric and ferrous heme of myoglobins [22,53]. Third, this protein is particularly amenable to study via NMR techniques [99] because of the presence of a well-resolved upfield-shifted methyl group resonance of PMe_3 coordinated to the metal atom in both oxidation states in the ^1H NMR spectra [52–55].

A mixture of oxidized and reduced horse heart myoglobin trimethylphosphine undergoes electron transfer in the slow exchange regime of the NMR time scale [100]. This was evident from measurements using saturation transfer techniques, as previously reported for cytochrome *c* [101,102]. Pre-irradiation at the frequency of the phosphine methyl resonance of myoglobin Fe(III) PMe_3, at a power level sufficient to abolish the resonance, caused a decrease of the intensity of the corresponding PMe_3 resonance of myoglobin Fe(II) [100]. Thus, myoglobin PMe_3 can be cycled between its two oxidation states by virtue of electron exchange. Inversion recovery techniques [101,102] were used to measure the spin–lattice relaxation time and to calculate the self-exchange rate constant (Fig. 11) [100]. The non-physiological electron transfer study in trimethylphosphine horse heart myoglobin between the two redox states Fe(II) and Fe(III) was measured as function of ionic strength, temperature and pH. In 0.1M potassium phosphate buffer, at pH 6.9 and 23 °C, the bimolecular rate constant for self-exchange for myoglobin PMe_3 is $3.1 \times 10^3 M^{-1} s^{-1}$. This rate constant for the protein studied here is remarkably similar to that previously reported for horse heart cytochrome *c* ($5.4 \times 10^3 M^{-1} s^{-1}$) [101] and for cytochrome b_5 ($2.6 \times 10^3 M^{-1} s^{-1}$) [103]. Furthermore, the rate under the same conditions but with added KCl to 0.7M was $3.7 \times 10^3 M^{-1} s^{-1}$. This increase is small and it was concluded that the rate is weakly dependant on ionic strength over this range of salt concentration [100]. The enthalpy of activation was 12.1 kcal mol^{-1}, and the entropy of activation was −1.2 cal mol^{-1} deg^{-1}.

The 300 MHz ^1H NMR spectrum of a mixture of reduced and oxidized PMe_3 complexes of cytochrome *c* is illustrated in Fig. 12 [88]. Clearly, the situation is similar to that which was previously observed with a mixture of trimethylphosphine metmyoglobin and trimethylphosphine myoglobin with slow chemical exchange. Thus, cytochrome *c* can also be cycled between its two oxidation states by virtue of electron exchange [87,88]. The rates of self-exchange electron transfer in the trimethylphosphine complex of cytochrome *c* have been measured by NMR over a large range of ionic strengths, using the same technique, i.e. inversion recovery [101,102]. The rate is $1.56 \times 10^4 M^{-1} s^{-1}$ at 23 °C ($\mu = 0.34$ M) at pH 6.9. The ionic strength dependence of the rate constant is treated by the van Leeuwen theory [104]. Extrapolation of the rate constant to infinite ionic strength gives a rate constant of

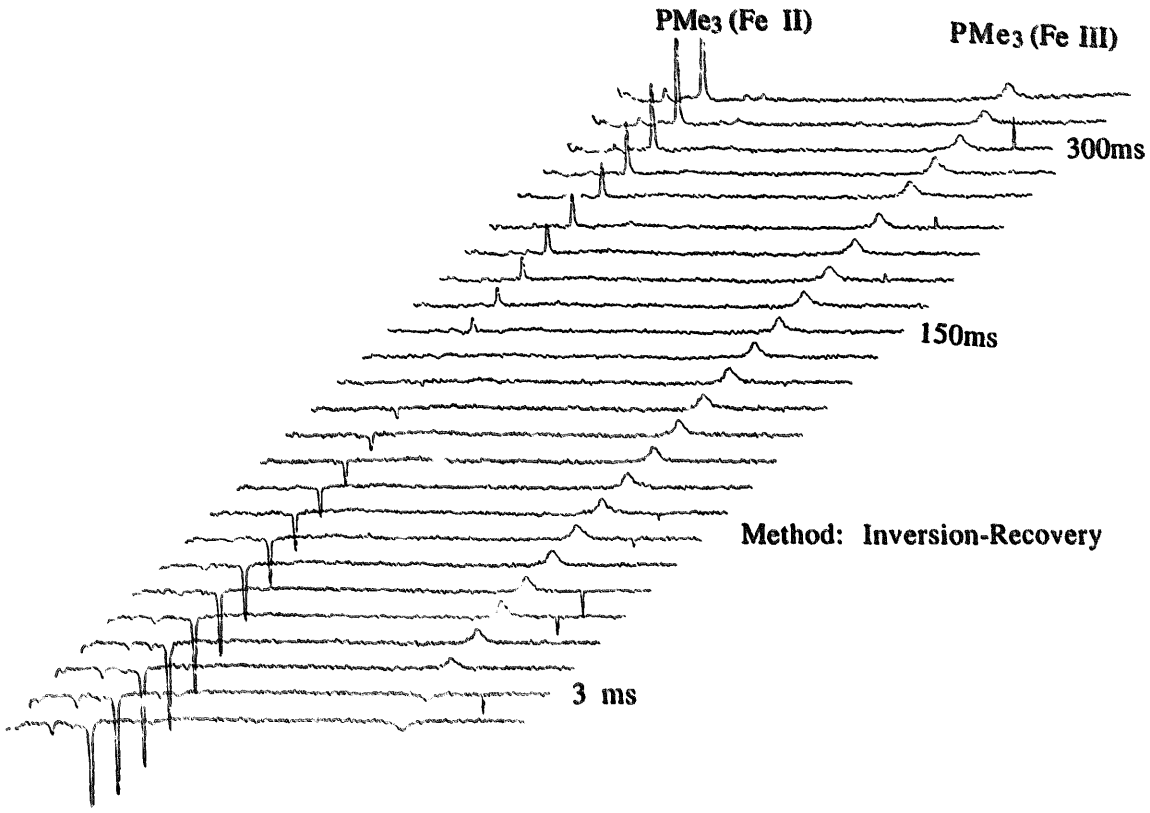

Fig. 11. Partially relaxed ^1H NMR spectra of horse heart myoglobin as a function of τ in a 180°–τ–90° T_1 inversion-recovery experiment.

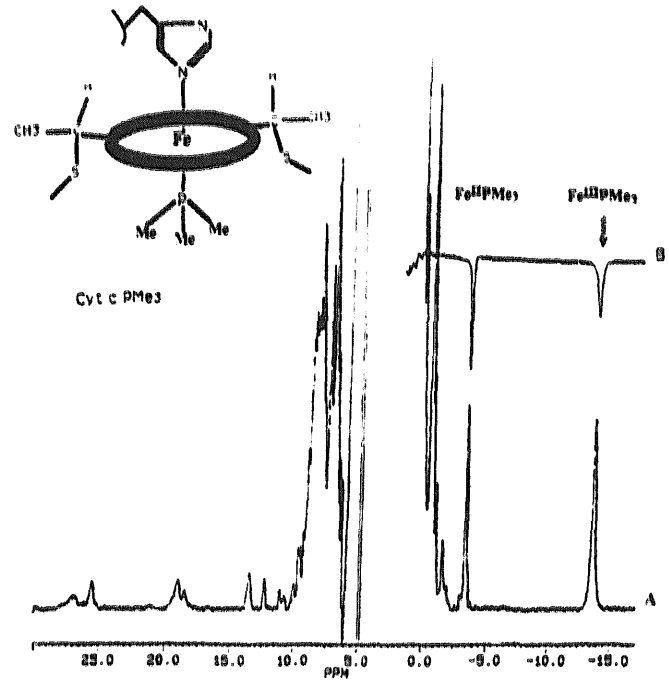

Fig. 12. ^1H NMR spectra of cytochrome *c* PMe_3 : A, ferric state; B, partially reduced state (Fe(III)/Fe(II) = 0.6).

$3.9 \times 10^5 M^{-1} s^{-1}$. This rate is compared with others reported for myoglobin and cytochrome b_5. The values for these systems range over two orders of magnitude with myoglobin PMe_3 [100] ≪cytochrome b_5 [103] <cytochrome $cPMe_3$ [88] <cytochrome c [101]. At this stage, it should be noted that the reorganization energy can be calculated from the rate constant at a given ionic strength and temperature. This approach was recently reported by Dixon et al. [101,103,105]. These authors have obtained reorganization energies of 0.72 eV for cytochrome c and 1.2 eV for cytochrome b_5 [103]. With the use of the Marcus formalism [95], the cytochrome c PMe_3 self-exchange rate constant can be expressed as:

$$k_{el} = SK_a \nu_n \kappa_{el} \exp(-\Delta G_r^*/RT)$$

where S is the steric factor, K_a is the association constant for formation of the precursor state from the two proteins, ν_n is the nuclear frequency factor, κ_{el} is the probability of electron tunneling and ΔG_r^* is the free energy of activation. Then the reorganization energy λ can be obtained through application of the following relationships according to the Marcus formalism:

$$\Delta G_r^* = (\lambda/4)[1 + \Delta G^{o'}/\lambda]^2$$

$$\Delta G^{o'} = \Delta G^o + w_p - w_r$$

where ΔG_r^* is the free energy of activation that is related to λ, to ΔG^o the free energy change of the reaction, and to the work of bringing the reactants (w_r) or products (w_p) to the mean separation distance in the electron transfer complex. For self-exchange reactions, ΔG^o is zero and $w_p = w_r$. Therefore, the energy of reorganization can be express as: $\lambda = 4\ \Delta G_r^*$ and the reorganization energy for the self-exchange reaction is 0.78 eV for cyt c PMe_3 [88] and 1.6 eV for $MbPMe_3$ [95].

In many hemoproteins, one edge of the heme iron–porphyrin prosthetic group is exposed to the protein surface, as for example cytochrome c, and thus the exposed heme edge has been proposed as the site for electron transfer [101,103]. Actually this situation is implicit in most of the discussion relevant to self-exchange electron transfer. In the absence of a three-dimensional structure for the PMe_3 ligated cytochrome c, it is not possible to rigorously define the geometry of the protein, in particular the modification in the heme pocket due to the presence of the phosphine ligand. Precisely how this different heme pocket (due to the bulky phosphine complexation) might transfer an electron cannot be determined only on the basis of these current studies. Moreover, the changes in the position of the amino acids on the distal side, due to the presence of the phosphine, may not be the single determining factor of the decrease of the rate at infinite ionic strength. For example, it has been recently demonstrated that Phe 82 does not contribute directly to electron transfer, when the thermodynamic driving force of the reaction is small (less than 100 mV) or zero, as it is the case for self-exchange reactions [106].

It is also of interest to determine the extent to which the coordination environment of hemoproteins is also dictated by the nature of the heme ring (heme a,b or c) and to what extent this may influence the rate of self-exchange electron transfer. Comparison of the rates of this cytochrome c PMe_3 with similar hemoproteins, as

myoglobin PMe_3 permits definition of this factor in greater detail [88]. Under infinite ionic strength, the rate was $7.5 \times 10^4 M^{-1} s^{-1}$. As myoglobin has more heme exposed to solvent than cytochrome *c* [107], the main question is: why does cytochrome *c* exchange electrons more rapidly than myoglobin since substitution of Met-80 by PMe_3 appears to influence only weakly the rearrangement barrier to electron transfer? To illustrate the foregoing point, Fig. 13 shows the heme pocket of four hemoproteins cyt. *c*, cyt. *c* PMe_3, cyt b_5 and Mb PMe_3 together with the values of the reorganization energies [88,103]. Clearly, there is a decrease in energy with an increase in the number of covalent links between the axial ligands and the heme ring. The gap is between cytochromes *c* and b_5 on the one hand, and myoglobin on the other. This behavior is not unique to self-exchange systems and has also been observed for intramolecular electron transfer reactions, as exemplified by different hemoproteins labelled with ruthenium complexes [107–109]. Among these four hemoproteins, cyt. *c* PMe_3 and Mb PMe_3 have two identical axial ligands and the iron coordination sphere differs mainly by the nature of the porphyrin ring. The heme moiety of cytochrome *c* is covalently linked by two thioether bonds at the vinyl groups and this greatly increases the stability of the system. In contrast, this does not occur in myoglobin, and the presence of only one link is not enough to maintain the stability, corresponding to a high reorganization energy and a low exchange rate. The very fast rate of self-exchange for cytochrome c_{551} is also

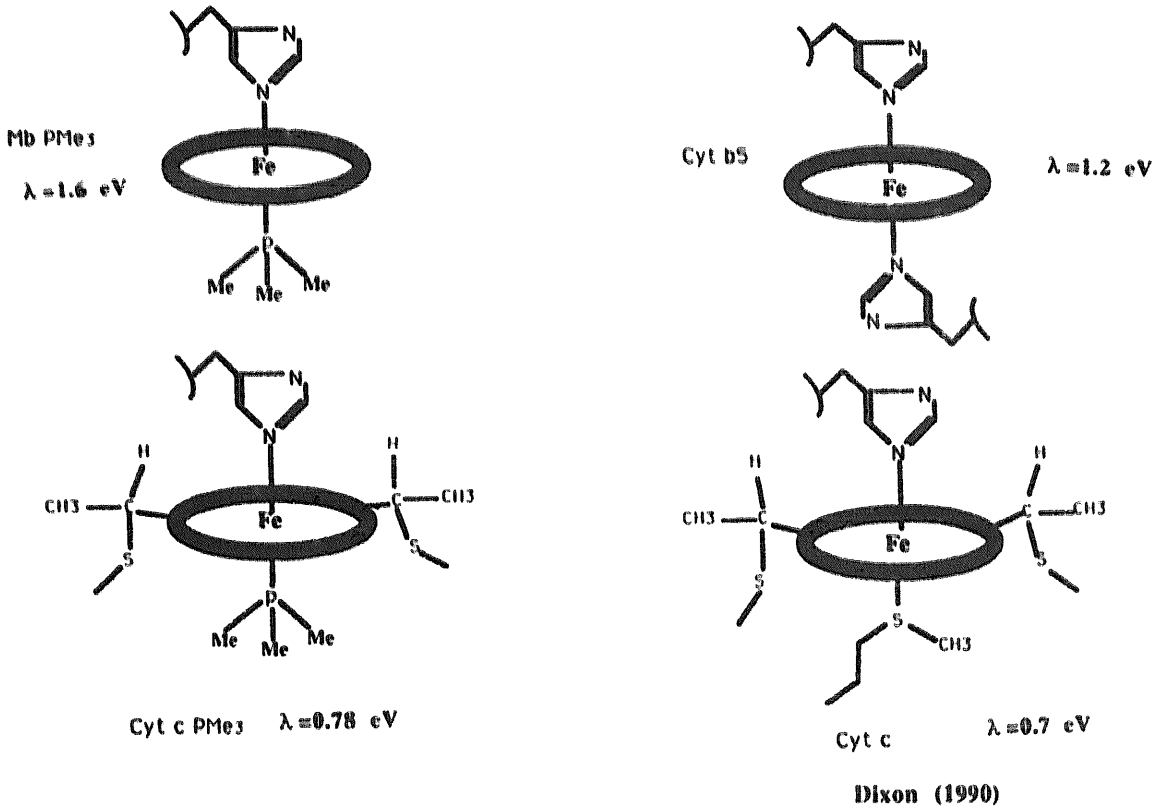

Fig. 13. Schematic iron coordination sphere displaying the heme-protein bonds, and calculated reorganization energies λ for Mb PMe_3, cyt b_5, cyt *c* PMe_3 and native cyt *c*.

explained as a small reorganizational energy for the protein [105]. In conclusion, these studies [88] suggest a role for the flexibility of the heme coordination sphere, in addition to the usual factors [95,110,111] in the modulation of biological electron transfer kinetics.

4.2.2. Hemoglobin

Despite their biological importance, there is little systematic experimental data on rates of bimolecular electron transfer with multiredox center hemoproteins [112,113]. Most of the studies with these particular systems have been focused on intramolecular [114–116] or interprotein complex [117] electron transfers.

Hemoglobins are particularly well-suited for detailed electron-transfer mechanistic investigation, because these proteins are well-characterized, including high-resolution crystal structures [118]. Furthermore, the availability of a convenient method for the preparation of mixed-metal hybrid hemoglobins [119] now permits a new approach to the study of heterosubunit interaction in hemoglobin.

An experimental investigation of the mechanism of electron transfer in trimethylphosphine complexed hemoglobin has also been performed [120]. The ^{1}H NMR

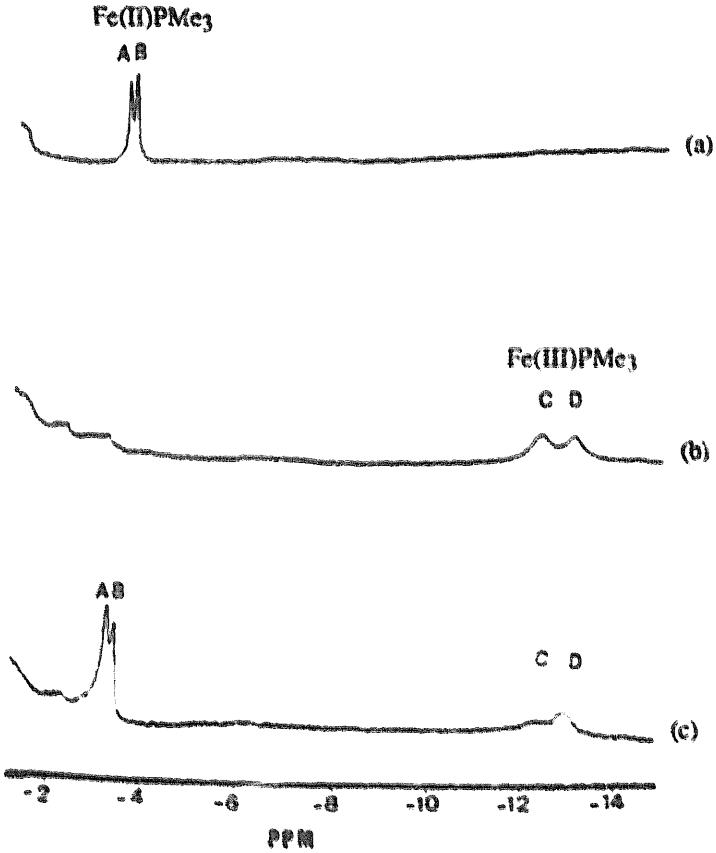

Fig. 14. The effect of metHbPMe$_3$ addition on the relative magnitude of the intensity of the PMe$_3$ methyl resonances of HbPMe$_3$ (high field portion of the spectra). Assignment of the methyl-group resonances: Fe(II)PMe$_3$, A (β chains) and B (α chains) and Fe(III)PMe$_3$, C (β chains) and D (α chains). (a) HbPMe$_3$, (b) metHbPMe$_3$, (c) mixture of human hemoglobin HbPMe$_3$/metHbPMe$_3$ in the ratio 65/35 in D_2O at 23 °C (pH 6.9).

spectrum recorded after addition of reduced (Fig. 14(a)) and oxidized (Fig. 14(b)) hemoglobin trimethylphosphine shows four resonances: two resonances from Fe(II) subunits [A (β chains) and B (α chains)] [18] and two resonances from Fe(III) subunits [C (β chains) and D (α chains)] [53] which are clearly seen in the upfield region (Fig. 14(c)). The α/β ratios for the ferric and ferrous states are 1.6 and 0.74, respectively, when 60% of the subunits are in the reduced state. Because the ratio between α chains and β chains are different from unity in both redox states, it was assumed that electron-exchange occurs between the different subunits. On this basis, the oxidation–reduction potentials of α/β chains are different, the electron affinity of the β chains being higher than that of the α chains. Such a difference in the redox potential has been previously reported with unligated native hemoglobin [121,122]. Using saturation transfer experiments with native and [Fe,Mn] hybrid Hb it was shown that both intra- and interchain electron transfers occur [112]. The mechanism of electron transfer might be intramolecular or (and) intermolecular. In order to obtain information on this point, the dependence of the inverse life-time ($1/\tau_{red}$) of the PMe_3 resonances of both chains, as a function of the concentration of exchanging species, was investigated. At constant ionic strength (0.1M phosphate buffer) and near neutral pH, the life-time of the ferrous state (rate of exchange process) shows first order decrease with the inverse of the ferrihemoglobin concentration. Therefore, intramolecular exchange has little (if any) influence on the rate of the reaction. Besides establishing an exchange of protein molecules between different oxidation states, the technique can also be used to measure the kinetics of the redox reactions [120]. However, because each subunit can be cycled between its two oxidation states by virtue of electron exchange with two different redox subunits, the exchange process is therefore:

$$[\alpha(III)PMe_3]+[\alpha(II)PMe_3] \underset{k_{-11}}{\overset{k_{11}}{\rightleftharpoons}} [\alpha(II)PMe_3]+[\alpha(III)PMe_3]$$

$$[\beta(III)PMe_3]+[\beta(II)PMe_3] \underset{k_{-22}}{\overset{k_{22}}{\rightleftharpoons}} [\beta(II)PMe_3]+[\beta(III)PMe_3]$$

$$[\alpha(II)PMe_3]+[\beta(III)PMe_3] \underset{k_{21}}{\overset{k_{12}}{\rightleftharpoons}} [\alpha(III)PMe_3]+[\beta(II)PMe_3]$$

where α(II) and α(III) are the α chains in respectively the ferrous and the ferric state; k_{11} and k_{12} are respectively, the self-exchange constant for the homosubunit reaction and the cross-exchange constant for the heterosubunit reaction.

The lifetimes of the two reduced species are described by the following equations:

$$\tau_{\alpha(II)} = \alpha(II)/k_{11}.[\alpha(II)].[\alpha(III)]+k_{12}.[\alpha(II)].[\beta(III)] \quad (5)$$

$$\tau_{\beta(II)} = \beta(II)/k_{22}.[\beta(II)].[\beta(III)]+k_{21}.[\beta(II)].[\alpha(III)] \quad (6)$$

Calculations based on ^1H NMR spectra and using the inversion-recovery method determined the rate constants to be $k_{11}=3200M^{-1}s^{-1}$ (α chains) and $k_{22}=2090M^{-1}s^{-1}$ (β chains) for self-exchange transfers, $k_{12}=1020M^{-1}s^{-1}$ ($[\alpha^2]+[\beta^3]$) and $k_{21}=430M^{-1}s^{-1}$ ($[\alpha^3]+[\beta^2]$) for interchain transfers. Application

of the Marcus relationship to cross reactions [95] yields $k_{12}=3830M^{-1}s^{-1}$ and $k_{21}=1730M^{-1}s^{-1}$ calculated values which are in good agreement with the NMR k_{12} and k_{21} values. Three factors (similar heme exposure, low driving force, small charge effect) were suggested to account for the good agreement between the observed and calculated constants indicating that all these electron transfers represent reactions by a single pathway with no evidence of configurationally-limited behavior [120].

4.3. Oxidation with P-450

The interaction of a lipophilic ligand with cytochrome P-450 will lead to an inhibition of substrate monooxygenation by either competition for the hydrophobic site close to the sixth coordination position or by preventing oxygen binding through complexation with the iron atom [123]. Some time ago, Mansuy et al. reported that diethylphenylphosphine can react with reduced microsomal cytochrome P-450 [50]. When tested in the O-dealkylation of 7-ethoxy-coumarin, diethylphenylphosphine was proved to be a potent inhibitor with a K_i-value of about $2\times10^{-6}M$ in freshly prepared microsomes. This mainly competitive inhibition of monooxygenase reactions by phosphines suggested that the lipophilic ligands and the substrates interact with the same hydrophobic pocket, quite close to the sixth coordination position of cytochrome P-450 [50].

The metabolism of two tertiary aromatic phosphines, diphenylmethylphosphine and 3-dimethylaminopropyldiphenylphosphine by rat liver microsomes was also studied and thus, found to be a functional probe of cytochrome P-450 [124]. The latter compound was found to be a mammalian central nervous system depressant and it thus represents one of a few examples of pharmacologically active trivalent phosphorous compounds [125]. These compounds were incubated with subcellular fractions of rat liver homogenates and found to be enzymatically converted to the corresponding phosphine oxides. Enzymatic activity was shown to be associated with the cytochrome P-450 mixed-function oxidases. [3-dimethylamino-propyl]diphenylphosphine was metabolized to yield a mixture of two products; the corresponding phosphine oxide and the N,P oxide. Since the oxygen atom of the mono-oxide is bonded to the phosphorous (not nitrogen), this result indicates that trivalent phosphorus is more susceptible to microsomal oxidation than nitrogen [124]

Although the interaction of phosphine (PH_3) itself with ferric hemes has been previously reported, in particular with cytochrome *c* and cytochrome oxidase [126], this ligand cannot be considered as a structural or a functional probe of hemoproteins and consequently this result will not be reviewed herein.

In conclusion, although phosphine ligands are generally considered as ligands for organometallic complexes, the study of their interactions with hemoproteins can be very useful for the understanding of the structure–function relationship of these metalloproteins. Phosphines are also more versatile than carbon monoxide in that they may serve as ligands to both ferric and ferrous heme iron of hemoproteins.

Acknowledgements

I thank my enthusiastic colleagues, past and present, for their crucial contributions to the work in my laboratory, in particular A. Bondon and P. Sodano who have taken this project in many creative directions.

References

[1] E. Antonini, M. Brunori, Hemoglobin and Myoglobin in their Reactions with Ligands, North-Holland, Amsterdam, 1971.
[2] I. Bertini, H.B. Gray, S.J. Lippard, J.S. Valentine, Bioinorganic Chemistry, University Science Books, Sausalito, CA, 1994.
[3] (a) W. Keim, B. Schwederski, Bioinorganic Chemistry: Inorganic Elements in the Chemistry of Life, An Introduction and Guide, Wiley, New York, 1994;(b) J.J.R. Frausto da Silva, R.J.P. Williams, The Biological Chemistry of The Elements, Oxford University Press, Oxford, 1991.
[4] C.A. Tolman, Chem. Rev. 77 (1977) 313.
[5] J.P. Collman, L.S. Hegedus, Principles and Applications of Organotransition Metal Chemistry, University Science Books, Mill Valley, 1980, p. 54.
[6] R.H. Crabtree, The Organometallic Chemistry of the Transition Metals, Wiley—Interscience, New York, 1988, p. 71.
[7] G. Wilkinson, Nature 168 (1951) 514.
[8] T.G. Spiro, J.M. Burke, J. Am. Chem. Soc. 98 (1976) 5482.
[9] D.V. Stynes, D. Fletcher, X. Chen, Inorg. Chem. 25 (1986) 3483.
[10] G. Simonneaux, P. Sodano, L. Toupet, J. Chem. Soc. Dalton Trans. (1988) 2615.
[11] L.M. Mink, J.R. Polam, K.A. Christensen, M.A. Bruck, F.A. Walker, J. Am. Chem. Soc. 117 (1995) 9329.
[12] T. Ohya, H. Morohoshi, M. Sato, Inorg. Chem. 23 (1984) 1303.
[13] R.M. Belani, B.R. James, D. Dolphin, S.T. Rettig, Can. J. Chem. 66 (1988) 2072.
[14] G.N. La Mar, J.D. Gaudio, J. Bioinorg. Chem. 2 (1977) 207.
[15] D.H. Chin, G.N. La Mar, A.L. Balch, J. Am. Chem. Soc. 102 (1980) 5947.
[16] W.R. Scheidt, C.A. Reed, Chem. Rev. 81 (1981) 543.
[17] L.K. Hanson, W.A. Eaton, S.G. Sligar, I.C. Gunsalus, M. Gouterman, C.R. Connell, J. Am. Chem. Soc. 98 (1976) 2672.
[18] G. Simonneaux, A. Bondon, C. Brunel, P. Sodano, J. Am. Chem. Soc. 110 (1988) 7637.
[19] B.B. Wayland, L.F. Mehne, J. Swartz, J. Am. Chem. Soc. 100 (1978) 2379.
[20] H. Scheer, J.J. Katz, in: K.M. Smith (Ed.), Porphyrins and Metalloporphyrins, Elsevier Scientific Publishing Company, Amsterdam, 1975, p. 399.
[21] T.R. Janson, J.J. Katz, Nuclear magnetic resonance spectroscopy of diamagnetic porphyrins, in: D. Dolphin (Ed.), The Porphyrins, Academic, New York, 1979, Vol. IV, pp. 1–59.
[22] A. Bondon, P. Petrinko, P. Sodano, G. Simonneaux, Biochim. Biophys. Acta 872 (1986) 163.
[23] L.M. Mink, K.A. Christensen, F.A. Walker, J. Am. Chem. Soc. 114 (1992) 6930.
[24] G.N. La Mar, J.S. de Ropp, V.P. Chacko, J.D. Satterlee, E. Erman, Biochim. Biophys. Acta 708 (1982) 317.
[25] J.R. Polam, J.L. Wright, K.A. Christensen, F.A. Walker, H. Flint, H. Winkler, M. Grodzicki, A.X. Trautwein, J. Am. Chem. Soc. 118 (1996) 5272.
[26] L. Toupet, N. Legrand, A. Bondon, G. Simonneaux, Acta Cryst. C50 (1994) 1014.
[27] C.A. Tolman, J. Am. Chem. Soc. 92 (1970) 2953.
[28] P. Sodano, thesis, Rennes, 1986.
[29] P. Sodano, G. Simonneaux, Inorg. Chem. 27 (1988) 3956.
[30] L. Toupet, P. Sodano, G. Simonneaux, Acta Cryst. C46 (1990) 1631.
[31] M. Guillemot, G. Simonneaux, J. Chem. Soc. Chem. Commun. (1995) 2093.

[32] C.A. Reed, T. Mashiko, S.P. Bentley, M.E. Kasner, W.R. Scheidt, K. Spartalian, G. Lang, J. Am. Chem. Soc. 101 (1979) 2948.
[33] H.M. Goff, E. Shimomura, J. Am. Chem. Soc. 102 (1980) 31.
[34] H.H. Ruf, P. Wende, J. Am. Chem. Soc. 99 (1977) 5499.
[35] H.H. Ruf, P. Wende, W. Ullrich, J. Inorg. Biochem. 11 (1979) 189.
[36] K.M. Kadish, L.A. Bottomley, Inorg. Chem. 19 (1980) 832.
[37] G.N. La Mar, F.A. Walker, J. Am. Chem. Soc. 95 (1973) 1782.
[38] J.D. Satterlee, G.N. La Mar, J. Am. Chem. Soc. 98 (1976) 2804.
[39] V.P. Chacko, G.N. La Mar, J. Am. Chem. Soc. 104 (1982) 7002.
[40] G.N. La Mar, F.A. Walker, in: The Porphyrin, D. Dolphin (Ed.), Academic, New York, 1979, Vol. IV, pp 57–161.
[41] F.A. Walker, U. Simonis, in: Biological Magnetic Resonance (1993), Berliner and Reuben (Eds.), Vol. 12, p. 132 and references therein.
[42] C.P.S. Taylor, Biochim. Biop' ys. Acta 491 (1977) 137.
[43] G. Palmer, in: A.B.P. Lever, H.B. Gray (Eds.), Iron Porphyrins, Part II, Addison-Wesley, Reading, 1983, p. 43.
[44] F.A. Walker, D. Reis, V. Balke, J. Am. Chem. Soc. 106 (1984) 6888.
[45] M.K. Safo, G.P. Gupta, C.T. Watson, U. Simonis, F.A. Walker, W.R. Scheidt, J. Am. Chem. Soc. 114 (1992) 7066.
[46] P.H. Rieger, Coord. Chem. Rev. 135/136 (1996) 203.
[47] (a) M.K. Safo, F.A. Walker, A.M. Raitsimring, W.P. Walters, D.P. Dolata, P.G. Debrunner, W.R. Scheidt, J. Am. Chem. Soc. 116 (1994) 7760;(b) F.A. Walker, H. Nasri, I. Turowska-Tyrk, K. Mohanrao, C.T. Watson, N.V. Shokhirev, P.G. Debrunner, W.R. Scheidt, J. Am. Chem. Soc. 118 (1996) 12 109.
[48] L. Toupet, P. Sodano, G. Simonneaux, Acta Cryst. C46 (1990) 1631.
[49] M. Guillemot, M.A. Pilard, J. Jordanov, L. Toupet, G. Simonneaux, submitted for publication.
[50] D. Mansuy, W. Duppel, H.H. Ruf, V. Ullrich, Z. Physiol. Chem. 355 (1974) 1341.
[51] M. Sono, J.H. Dawson, L.P. Hager, Inorg. Chem. 24 (1985) 4339.
[52] A. Bondon, P. Sodano, G. Simonneaux, C.T. Craescu, Biochim. Biophys. Acta 914 (1987) 289.
[53] G. Simonneaux, A. Bondon, P. Sodano, Inorg. Chem. 26 (1987) 3636.
[54] G. Simonneaux, A. Bondon, P. Sodano, S. Sinbandhit, Biochim. Biophys. Acta 999 (1989) 42.
[55] G. Simonneaux, A. Bondon, P. Sodano, Biochim. Biophys. Acta 1038 (1990) 199.
[56] C. Brunel, A. Bondon, G. Simonneaux, Eur. J. Biochem. 214 (1993) 405.
[57] L.A. Andersson, M. Sono, J.H. Dawson, Biochim. Biophys. Acta 748 (1983) 341.
[58] M. Sono, J.H. Dawson, K. Hall, L.P. Hager, Biochemistry 25 (1986) 347.
[59] R.E. White, M.J. Coon, J. Biol. Chem. 257 (1982) 3073.
[60] V. Ullrich, H.H. Ruf, P. Wende, Croat. Chem. Acta 49 (1977) 213.
[61] M. Sono, L.P. Hager, J.H. Dawson, Biochim. Biophys. Acta 1078 (1991) 351.
[62] R.E. Dickerson, I. Geis, The Structure and Action of Proteins, The Bejamin/Cummings Publishing Company, Inc., Menlo Park, 1969.
[63] E. Antonini, M. Brunori, J. Wyman, Biochemistry 4 (1965) 545.
[64] A. Kumar, R.R. Ernst, K. Wüthich, Biochem. Biophys. Res. Commun. 95 (1980) 1.
[65] K. Wüthrich, NMR of Proteins and Nucleic Acids, Wiley and Sons, New York, 1986.
[66] D. Marion, K. Wütrich, Biochem. Biophys. Res. Commun. 113 (1983) 967.
[67] C. Wagner, K. Wütrich, J. Magn. Reson. 33 (1979) 675.
[68] S. Ramaprasad, R.D. Johnson, G.N. La Mar, J. Am. Chem. Soc. 106 (1984) 5330.
[69] A. Mayer, S. Ogawa, R.G. Shulman, T. Yamane, J.A.S. Cavaleiro, A.M. Rocha Gonsalves, G.W. Kenner, K.M. Smith, J. Mol. Biol. 86 (1974) 5330.
[70] G.N. La Mar, D.B. Viscio, K.M. Smith, W.S. Caughey, M.L. Smith, J. Am. Chem. Soc. 100 (1978) 8085.
[71] G.N. La Mar, L.D. Budd, K.M. Smith, Biochim. Biophys. Acta 622 (1980) 210.
[72] T.G. Traylor, A.P. Berzinis, J. Am. Chem. Soc. 102 (1980) 2844.
[73] R.G. Shulman, S.H. Glarum, M. Karplus, J. Mol. Biol. 57 (1971) 93.

[74] G.N. La Mar, L.D. Budd, D.G. Viscio, K.M. Smith, K.C. Laugry, Proc. Natl. Acad. Sci. USA 75 (1978) 5755.
[75] I. Morishima, S. Neya, T. Inubishi, T. Yonezawa, T. Iizuka, Biochim. Biophys. Acta 534 (1978) 307.
[76] N. Legrand, thesis, University of Rennes 1, 1994.
[77] A. Bondon, N. Legrand, G. Simonneaux, G. Hui Bon Hoa, Workshop on Structure–Function Relationship in Peroxidases and Cytochromes 450, Le Bishenberg, France, June 1994.
[78] P. George, S.T. Glauser, A. Schejter, J. Biol. Chem. 242 (1967) 1690.
[79] A. Schejter, I.J. Aviram, J. Biol. Chem. 245 (1970) 1552.
[80] N. Sutin, J.K. Yandell, J. Biol. Chem. 247 (1972) 6932.
[81] R. Bechtold, M.B. Gardinner, A. Kazmi, B. Van Hemelrick, S.S. Isied, J. Phys. Chem. 90 (1986) 3800.
[82] W. Shao, Y. Yao, G. Liu, W. Tang, Inorg. Chem. 32 (1993) 6112.
[83] W. Shao, H. Sun, Y. Yao, W. Tang, Inorg. Chem. 34 (1995) 680.
[84] E. Margoliash, A. Schejter, Adv. Protein Chem. 21 (1966) 113.
[85] A. Schejter, B. Plotkin, Biochem. J. 255 (1988) 353.
[86] A. Schejter, B. Plotkin, I. Vig, FEBS Letters 280 (1991) 199.
[87] N. Legrand, A. Bondon, G. Simonneaux, A. Schejter, Magn. Reson. Chem. 31 (1993) S23.
[88] N. Legrand, A. Bondon, G. Simonneaux, Inorg. Chem. 35 (1996) 1627.
[89] A. Schejter, I. Aviram, Biochemistry 8 (1969) 149.
[90] C.A. Tolman, J. Am. Chem. Soc. 92 (1970) 2956.
[91] R. Benesch, R.E. Benesch, Biochem. Biophys. Res. Commun. 26 (1967) 162.
[92] A. Bondon, G. Simonneaux, Biophys. Chem. 37 (1990) 407.
[93] M.F. Perutz, Nature (London) 228 (1970) 726.
[94] A. Brozozowski, A. Derewenda, E. Dodson, M. Grabowski, R. Liddington, T. Skarzynski, D. Valley, Nature (London) 307 (1984) 74.
[95] R.A. Marcus, N. Sutin, Biochim. Biophys. Acta 811 (1985) 265.
[96] K. Tsukahara, T. Okazawa, H. Takahashi, Y. Yamamoto, Inorg. Chem. 25 (1986) 4756.
[97] K. Hegetschweiler, P. Saltman, C. Dalvit, P.E. Wright, Biochim. Biophys. Acta 912 (1987) 384.
[98] S.V. Evans, G.D. Brayer, J. Biol. Chem. 263 (1988) 4263.
[99] I. Bertini, C. Luchinat, NMR of Paramagnetic Molecules in Biological Systems, The Bejamin/Cummings Publishing Company, Inc., Menlo Park, 1986.
[100] C. Brunel, A. Bondon, G. Simonneaux, Biochim. Biophys. Acta 1101 (1992) 73.
[101] D.W. Dixon, X. Hong, S.E. Woehler, Biophys. J. 56 (1989) 339.
[102] R.K. Gupta, A.S. Mildvan, Methods Enzymol. 54 (1978) 171.
[103] D.W. Dixon, X. Hong, S.E. Woehler, A.G. Mauk, B.P. Sishta, J. Am. Chem. Soc. 112 (1990) 1082.
[104] J.W. Van Leeuwen, Biochim. Biophys. Acta 743 (1983) 408.
[105] D.W. Dixon, X. Hong, Adv. Chem. Ser. 226 (1990) 162.
[106] D.W. Concar, D. Witford, G. Pielak, R.P.J. William, J. Am. Chem. Soc. 113 (1991) 2401.
[107] J.R. Winkler, D.G. Nocera, K.M. Yocom, E. Bordignon, H.B. Gray, J. Am. Chem. Soc. 104 (1982) 5798.
[108] I. Moreira, J. Sun, M.O.K. Cho, J.F. Wishart, S.S. Isied, J. Am. Chem. Soc. 116 (1994) 8396.
[109] M.J. Therien, J. Chang, A.L. Raphael, B.E. Bowler, H.B. Gray, Struct. Bonding 75 (1991) 109.
[110] Electron transfer, in: Inorganic, Organic and Biological systems, J.R. Bolton, N. Mataga, G. McLendon (Eds.), Adv. Chem. Ser. 228 (1991).
[111] J.R. Winkler, H.B. Gray, Chem. Rev. 92 (1992) 369.
[112] S.A. Schichman, H.B. Gray, J. Amer. Chem. Soc. 103 (1981) 7794.
[113] H. Santos, J.G. Moura, I. Moura, J. LeGall, A.V. Xavier, Eur. J. Biochem. 141 (1984) 283.
[114] S.E. Peterson-Kennedy, J.L. McGourty, J.A. Kalweit, B.M. Hoffman, J. Am. Chem. Soc. 108 (1986) 1739.
[115] A.W. Axup, M. Albin, S.L. Mayo, R.J. Crutchley, H.B. Gray, J. Am. Chem. Soc. 110 (1988) 435.
[116] D.R. Casimiro, L.L. Wong, J.L. Colon, T.E. Zewert, J.H. Richards, I.-J. Chang, J.R. Winkler, H.B. Gray, J. Am. Chem. Soc. 115 (1993) 1485.
[117] K.P. Simolo, G.L. McLendon, M.R. Mauk, A.G. Mauk, J. Am. Chem. Soc. 106 (1984) 5012.
[118] B. Shaanan, J. Mol. Biol. 171 (1983) 31 and references therein.

[119] A. Arnone, P. Rogers, N.V. Blough, J.L. McGourty, B.M. Hoffman, J. Mol. Biol. 188 (1986) 693.
[120] C. Brunel, A. Bondon, G. Simonneaux, J. Am. Chem. Soc. 116 (1994) 11827.
[121] R. Banerjee, R. Cassoly, J. Mol. Biol. 42 (1969) 337.
[122] M. Brunori, A. Alfsen, U. Saggese, E. Antonini, J. Wyman, J. Biol. Chem. 243 (1968) 2950.
[123] V. Ullrich, K.H. Schnabel, Drug. Metab. Disposition 1 (1973) 176.
[124] R.A. Wiley, L.A. Sternson, H.A. Sasame, J.R. Gillette, Biochemical Pharmacology 21 (1972) 3235.
[125] R.A. Wiley, H.N. Godwin, J. Pharm. Sci. 54 (1965) 1063.
[126] K.P. Kashi, W. Chefurka, Pesticide Biochem. Physiol. 6 (1976) 350.